AD-A188 910 TIME-DEPENDENT SLOW-TIME-SCALE THEORY OF FREE-RUNNING AND PHASE-LOCKED GYROTRON OSCILLATORS(U) NAVAL RESEARCH LAB WASHINGTON DC A W FLIFLET ET AL. 19 JAN 88 1/1

UNCLASSIFIED NRL-MR-6064 F/G 14/2 NL

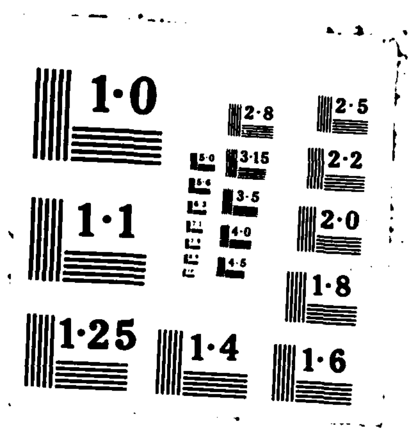
1·0
2·8
2·5
3·15
2·2
3·5
1·1
4·0
2·0
4·5
1·8
1·25
1·4
1·6

Naval Research Laboratory
Washington, DC 20375-5000

DTIC FILE COPY

NRL Memorandum Report 6064

Time-Dependent Slow-Time-Scale Theory of Free-Running and Phase-Locked Gyrotron Oscillators

A. W. FLIFLET, R. C. LEE*
W. M. MANHEIMER, AND E. OTT†

High Power Electromagnetic Radiation Branch
Plasma Physics Division

**JAYCOR, Inc.*
Vienna, VA 22180

†*Electrical Engineering Department*
University of Maryland
College Park, MD 20742

January 19, 1988

This work was supported by the Office of Innovative Science and Technology of the Strategic Defense Initiative Organization under a contract administered by the Harry Diamond Laboratories.

SECURITY CLASSIFICATION OF THIS PAGE

REPORT DOCUMENTATION PAGE

Form Approved OMB No 0704-0188

1a REPORT SECURITY CLASSIFICATION UNCLASSIFIED	1b RESTRICTIVE MARKINGS
2a SECURITY CLASSIFICATION AUTHORITY	3 DISTRIBUTION/AVAILABILITY OF REPORT Approved for public release; distribution unlimited.
2b DECLASSIFICATION/DOWNGRADING SCHEDULE	
4 PERFORMING ORGANIZATION REPORT NUMBER(S) NRL Memorandum Report 6064	5 MONITORING ORGANIZATION REPORT NUMBER(S) 47-2700-00
6a NAME OF PERFORMING ORGANIZATION Naval Research Laboratory 6b OFFICE SYMBOL (If applicable) 4740	7a NAME OF MONITORING ORGANIZATION
6c. ADDRESS (City, State, and ZIP Code) Washington, DC 20375-5000	7b ADDRESS (City, State, and ZIP Code)
8a. NAME OF FUNDING/SPONSORING ORGANIZATION Strategic Defense Initiative Organization/IST 8b OFFICE SYMBOL (If applicable)	9 PROCUREMENT INSTRUMENT IDENTIFICATION NUMBER
8c. ADDRESS (City, State, and ZIP Code) Washington, DC 20301-7100	10 SOURCE OF FUNDING NUMBERS PROGRAM ELEMENT NO: 66000A PROJECT NO: DN156-218 TASK NO: 0 WORK UNIT ACCESSION NO: 47-2700-00

11 TITLE (Include Security Classification)
Time-Dependent Slow-Time-Scale Theory of Free-Running and Phase-Locked Gyrotron Oscillators

12 PERSONAL AUTHOR(S)
Fliflet, Arne W., Lee*, Robert C., Manheimer, Wallace M., Ott**, Edward

13a TYPE OF REPORT	13b TIME COVERED	14 DATE OF REPORT (Year, Month, Day)	15 PAGE COUNT
Interim	FROM 10/86 TO 9/87	1988 January 19	35

16 SUPPLEMENTARY NOTATION
*JAYCOR, Inc., Vienna, VA 22180
**Electrical Engineering Department, University of Maryland, College Park, MD 20742

17 COSATI CODES			18 SUBJECT TERMS (Continue on reverse if necessary and identify by block number)
FIELD	GROUP	SUB-GROUP	High Power, Phase-Locked Gyrotron Oscillators, Intense Relativistic Electron Beams, Pulse-Line Accelerator, Interacting Modes, Short Pulselength, Voltage Risetime

19 ABSTRACT (Continue on reverse if necessary and identify by block number)

A time-dependent slow-time-scale theory is developed for the analysis of high power, pulsed gyrotrons. Calculations are carried out to simulate the operation of a 35 GHz high voltage gyrotron. Both free-running and phase-locked oscillator configurations are examined, and the effect of a voltage ripple is shown.

20 DISTRIBUTION/AVAILABILITY OF ABSTRACT ☒ UNCLASSIFIED/UNLIMITED ☐ SAME AS RPT ☐ DTIC USERS	21 ABSTRACT SECURITY CLASSIFICATION UNCLASSIFIED
22a NAME OF RESPONSIBLE INDIVIDUAL Arne W. Fliflet	22b TELEPHONE (Include Area Code) 202 767-2469 22c OFFICE SYMBOL 4740

DD Form 1473, JUN 86 Previous editions are obsolete SECURITY CLASSIFICATION OF THIS PAGE

S/N 0102-LF-014-6603

CONTENTS

TIME-DEPENDENT SLOW-TIME-SCALE THEORY OF FREE-RUNNING AND PHASE-LOCKED GYROTRON OSCILLATORS

I. INTRODUCTION

There is currently considerable interest in the development of high power phase-locked gyrotron oscillators. These devices have the potential to combine the high efficiency and power associated with oscillators with the coherence and phase control properties associated with amplifiers. Although previous theoretical work on gyrotron operation[1-8] has been successfully applied to the development of cw devices for heating of tokamak plasmas, the investigation of phase-locked gyrotron operation, particularly involving pulse-line accelerator driven devices, presents a new challenge to the theorist. These devices, based on intense relativistic electron beams, are characterized by short pulselengths and voltage risetime and ripple effects which can prevent the establishment of a steady-state equilibrium. A consideration of non-stationary operation is also involved in the investigation of conditions for phase-locked operation. Time-dependent effects can be studied using a particle-in-cell simulation code of the type developed by Lin and co-workers[9]. In this work an alternative slow-time-scale approach is used to obtain a relatively simple, economical analysis of the time-dependent, nonlinear dynamics of pulsed gyrotrons.

The time-dependent theory of gyrotrons has been considered by Nusinovich and co-workers[10,11], mainly in the context of

Manuscript approved September 28, 1987.

multimode operation and mode stability. A time multimode theory of quasi-optical gyrotrons has been developed by Bondeson et al.[12]. Early work on mode selection and phase-locking of vacuum tube oscillators was carried out by Van der Pol[13] and Adler[14]. An analytical theory of the conditions for phase-locking gyrotrons has been presented by Manheimer[15,16]. The emphasis in the present work is on the modeling of transient effects in gyrotrons whose pulse length is only a few times longer than the characteristic risetime of cavity fields. The approach is developed for the case of several interacting modes with closely spaced frequencies and interacting at the same harmonic of the cyclotron frequency. Calculations are presented for single mode operation of relativistic gyrotron with parameters similar to an experimental device under test at the Naval Research Laboratory[17]. Both free-running and phase-locked operation are considered. The phase-locking signal is introduced via a prebunched beam. The effect of a voltage ripple is investigated. The possibility of phase-locked operation in the presence of voltage ripple - an important issue for proposed NRL experiments - is demonstrated. Calculations for multimode operation will be the subject of future work.

The time theory of gyrotron oscillators derived in this work is based on slow-time-scale equations for the electron motion similar to those used in steady-state models[7,18,19]. Slow-time-scale equations for the cavity rf field amplitude are obtained by expressing the time-dependant behavior relative to a reference frequency ω_o which is close to the operating frequency ω. The next section of this paper contains an outline of the theoretical approach. The third section contains the results of calculations and the last section presents some conclusions drawn from this research.

II. THEORY

Consider a gyrotron with a cylindrical resonator and a thin annular beam. The electrons follow helical trajectories in the applied axial magnetic field about guiding centers located at a radius R_o from the symmetry axis. The electron beam interacts with one or more resonator modes, which are assumed to be TE modes with closely spaced oscillation frequencies. It is convenient to look at time effects which remain after a reference frequency ω_o has been factored out. These effects are characterized by time scales which are much longer than the wave period and are incorporated in time mode amplitudes $A_n(t)$. The total transverse electric field is expressed in the form

$$E_t = \sum_{n=1}^{N} A_n(t)h_n(z)e_n(r,\theta;z)\exp(-i\omega_o t) \tag{1}$$

where e_n is a transverse mode vector function defined in Ref. 18, and $h_n(z)$ is an axial profile function which satisfies the Helmholtz equation;

$$\left[\frac{d^2}{dz^2} + k_{zn}^2\right]h_n(z) = 0 \tag{2}$$

The function $P_n = h_n e_n$ is an eigenfunction of the empty resonator in the single transverse mode approximation with eigenfrequency ω_{no}. Thus the present formulation neglects beam loading effects on the mode axial profile. N is the number of interacting modes. The slowly varying mode amplitudes have the form:

$$A_n(t) = f_n(t)e^{-i\psi_n(t)} \tag{3}$$

The phase derivative $\psi_n' = d\psi_n/dt$ corresponds to the frequency difference between the mode oscillation frequency ω_n and ω_o. The transverse electric field satisfies the wave equation:

$$\nabla^2 \mathbf{E}_t - \frac{1}{c^2}\frac{\partial^2 \mathbf{E}_t}{\partial t^2} = \mu_o \frac{\partial \mathbf{J}_t}{\partial t} \tag{4}$$

where $\mathbf{J}_t$ is the transverse ac current density, c is the speed of light and μ_o is the permeability of free space. MKS units are used throughout except as noted. Substituting Eq.(1) into Eq.(4), introducing a mode Q factor, Q_n, to account for diffraction and ohmic losses, and noting that $dA_n/dt \ll \omega_o A_n$ one obtains

$$\sum_{n=1}^{N} e^{-i\omega_o t}\left[(\omega_o^2 - \omega_{no}^2)A_n + \frac{i\omega_{no}^2}{Q_n}A_n + 2i\omega_o \frac{dA_n}{dt}\right]h_n e_n = c^2 \mu_o \frac{\partial J_t}{\partial t} \tag{5}$$

where ω_{no} is the empty resonator eigenfrequency for the nth mode. Multiplying Eq.(5) on both sides by $(h_n e_n)^*$, integrating over the cavity volume and applying the orthogonality properties of the transverse vector functions[18] leads to the mode excitation equation:

$$\left[\frac{d}{dt} + \frac{\omega_o}{2Q_n} - i(\omega_o - \omega_{no})\right]A_n(t) = -\frac{ic^2\mu_o}{2N_n\omega_o}\int_V dzda\ h_n^* e_n^* \cdot \frac{\partial J_t}{\partial t} e^{i\omega_o t} \tag{6}$$

where N_n is the axial mode normalization integral:

$$N_n = \int_o^L dz\ |h_n(z)|^2 \tag{7}$$

To evaluate the right hand side of Eq.(6) the rf current density is written in the approximate form[7]:

$$J_t = J_{\omega_o} \exp(-i\omega_o t) \tag{8}$$

where

$$J_{\omega_o} = \int_0^{2\pi} d(\omega_o t) J_t\ e^{i\omega_o t} \tag{9}$$

Introducing the normalized frequency shift $\delta_n = (\omega_o - \omega_{no})/\omega_o$ and time $\tau = \omega_o t$ and substituting Eq.(8) into Eq.(6) leads to:

$$\left[\frac{d}{d\tau} + \frac{1}{2Q_n} - i\delta_n\right]A_n(\tau) = -\frac{c^2\mu_o}{2N_n\omega_o}\int_V dzda\ h_n^* e_n^* \cdot J_{\omega_o} e^{-i\psi_n} \tag{10}$$

To calculate the ac current density, the interaction with the electron beam is treated in the single particle approximation. A considerable simplification of the general time-dependent problem results if one uses the fact that the characteristic rise-time of fields in the resonator is much longer than the electron transit time in the cavity. In this case one can use a quasi-steady-state approximation in which the electron trajectories are calculated for rf fields with fixed amplitude, [illegible](τ_o), and linearized phase, $\psi_n \simeq \psi_n'(\tau_o)(\tau-\tau_o)$. The slow-time-scale nonlinear electron equations of motion for a particular harmonic are readily deduced from previous steady-state analyses[7,18] and are given by:

$$\frac{du_t}{d\bar{z}} = -\frac{\gamma}{u_z}\sum_{n=1}^{N} F_n J_s'(\bar{k}_n \bar{r}_L)\ \mathrm{Re}\left[\left(h_n + i\frac{u_z}{\gamma\bar{\omega}_o}\frac{dh_n}{d\bar{z}}\right)e^{-i[\Lambda+\psi_n-(m_n-s)\Xi_o]}\right] \tag{11a}$$

$$\frac{d\Lambda}{d\bar{z}} = -\frac{s\gamma}{u_z u_t}\sum_{n=1}^{N} F_n \frac{sJ_s(\bar{k}_n \bar{r}_L)}{\bar{k}_n \bar{r}_L}\mathrm{Re}\left[\left(h_n + i\frac{u_z}{\gamma\bar{\omega}_o}\frac{dh_n}{d\bar{z}} - \frac{\bar{\omega}_{n\,o}^2 u_t^2}{s\bar{\Omega}\bar{\omega}_o\gamma}h_n\right) e^{-i[\Lambda+\psi_n-(m_n-s)\Xi_o]}\right] + \bar{\omega}_o\left(1 - \frac{s\bar{\Omega}\gamma_o}{\bar{\omega}_o\gamma}\right) \tag{11b}$$

$$\frac{du_z}{d\bar{z}} = \frac{u_t}{u_z\bar{\omega}_o}\sum_{n=1}^{N} F_n J_s'(\bar{k}_n \bar{r}_L)\mathrm{Re}\left[i\frac{dh_n}{d\bar{z}}\ e^{-i[\Lambda+\psi_n-(m_n-s)\Xi_o]}\right] \tag{11c}$$

where $u_t = \gamma v_t/c$ is the normalized transverse momentum amplitude, $u_z = \gamma v_z/c$ is the normalized axial momentum, Λ is a slowly varying transverse momentum phase, s is the harmonic number, m_n is the mode azimuthal index, γ is the relativistic mass ratio, k_n is the mode transverse wavenumber, r_L is the Larmor radius of the orbit, J_s (J_s') is (the derivative of) a regular Bessel function, Ω is the relativistic cyclotron frequency correspondong to the input beam energy, Ξ_o is the orbit guiding center azimuthal angle, and F_n is the normalized rf field amplitude:

$$F_n = \frac{|e|}{m_e c^2} \frac{J_{m_n - s}(k_n R_o)}{\sqrt{[\pi(1-m_n^2/x_n'^2)]}\, J_{m_n}(x_n')} f_n \qquad (12)$$

Quantities with a "-" have been normalized according to: $\bar{z}=z/r_{wo}$, $\bar{r}_L = r_L/r_{wo}$, $\bar{\Omega}=\Omega r_{wo}/c$, $\bar{\omega}_o = \omega_o r_{wo}/c$, and $\bar{k}_n = k_n r_{wo}$. R_o denotes the orbit guiding center radius, e is the electron charge, m_e is the electron mass, x_n' is a zero of J_m' for the mode n, and r_{wo} is an arbitrary normalization length usually chosen to be a representative cavity wall radius.

The ac current density is obtained by integrating Eqs.(11) for an appropriate set of initial conditions at the cavity input at z_o. For a cold, phase-mixed electron beam: $u_t(z_o)=u_{to}$, $u_z(z_o)=u_{zo}$, and $\Lambda(z_o)=\Lambda_o$ is uniformly distributed in the interval $[0,2\pi]$. The case of an electron beam prebunched by passage through a bunching cavity driven at a frequency ω_o can be modeled by an initial phase angle distribution of the form:

$$\Lambda_o = \Theta_o + q_B \sin\Theta_o - \Phi_o \tag{13}$$

where Θ_o is uniformly distributed in the interval $[0,2\pi]$, q_B is the bunching parameter, and Φ_o is an initial phase. For an annular beam, Eqs.(11) are averaged with respect to Ξ_o. For a thin annular beam the transverse ac current density is given by

$$\mathbf{J}_t = -\frac{I_o}{v_z}\mathbf{v}_t \tag{14}$$

Substitution of Eqs.(14) and (9) into Eq.(10) leads to the following equations for the mode amplitude and phase:

$$\frac{dF_n}{d\tau} = \mathrm{Re}\left(I\int d\bar{z} h_n^* \left\langle \frac{u_t}{u_z} J_s'(\bar{k}_n \bar{r}_L) e^{i[\Lambda+\psi_n-(m_n-s)\Xi_o]} \right\rangle_{\Lambda_o,\Xi_o} \right) - \frac{F_n}{2Q_n} \tag{15a}$$

$$\frac{d\psi_n}{d\tau} = -\delta_n - \mathrm{Im}\left(I\int d\bar{z} h_n^* \left\langle \frac{u_t}{u_z} J_s'(\bar{k}_n \bar{r}_L) e^{i[\Lambda+\psi_n-(m_n-s)\Xi_o]} \right\rangle_{\Lambda_o,\Xi_o} \right) \tag{15b}$$

where I is the normalized current parameter:

$$I = \frac{|e|\mu_o}{m_o c\bar{\omega}_o} \frac{r_{wo} J^2_{m-s}(k_n R_o)}{\pi(1-m^2/x_n'^2) J^2_m(x_n') N_n} I_o \tag{16}$$

and $\langle\ \rangle_a$ denotes an average with respect to the variable a. The time behavior of a free-running or driven gyrotron oscillator is obtained by solving Eqs.(15) together with (11) subject to appropriate initial conditions as discussed above. When the phase ψ_n of a driven oscillator (via beam prebunching) converges to a constant value, the oscillator is said to be phase-locked. The locking frequency is ω_o in the present formulation. When the interaction occurs with only a single circularly polarized mode, the ac current density averaged with respect to Λ_o is independent of the guiding center azimuthal position so that the average with to Ξ_o may be omitted.

III. RESULTS

Calculations have been carried for a high voltage 35 GHz gyrotron configuration similar to the NRL experiment recently reported by Gold et al.[17]. The peak voltage and current of the annular beam are taken to be 650 kV and 1.5 kA, respectively. The beam guiding center radius is R_o=1.16 cm, the cavity radius is 1.6 cm, and the longitudinal profile of the cavity fields is assumed to be sinusoidal with length 4 cm. The operating mode is the TE_{621} circular mode with polarization counter-rotating to the beam rotation. The beam pitch ratio $\alpha \equiv v_t/v_z = 1$. The cavity Q factor Q=250. The applied magnetic field is 2.4 Tesla. Spreads in beam guiding center and pitch ratio are neglected as are space-charge effects. In these calculations the cavity is seeded with low amplitude rf fields (1 kV/cm at the beam in the present case). The results of calculations for free-running and phase-locked oscillator operation are presented below. The effect of a voltage ripple is shown.

The first set of calculations correspond to an idealized 50 nsec voltage pulse with a 3 nsec rise from 75% of peak to peak voltage and no ripple. The beam current and pitch ratio are assumed to vary linearly with voltage and as $V^{1.33}$, respectively, during the voltage rise up to the maximum values given above. Results for the free-running oscillator are shown in Figures 1 (a)-1(c). These Figures show, respectively, the electronic efficiency, operating frequency, and rf phase of the oscillator plotted as a function of time. Figure 1(b) plots the shift in operating frequency ω relative to ω_o which is taken to be the the cold cavity eigenfrequency (which is close to 35 GHz). These plots indicate that steady-state operation is achieved after about 8 nsec. The steady-state efficiency is 17.7%, corresponding to an output power of 173 MW, and the steady-state frequency shift $\delta_{FR}=(\omega_{FR}-\omega_o)/\omega_o$ due to beam loading is 5.5×10^{-4} which corresponds to 19.2 MHz. This frequency shift leads to a linearly increasing rf phase with time as shown in Figure 1(c).

Results for an oscillator driven via a prebunched beam are given in Figures 2(a)-2(c). The beam is modulated at a frequency ω_o and the modulation amplitude is modeled by the bunching parameter $q_B=0.5$. An estimate for the locking signal power required to obtain a beam with $q_B=0.5$ is given below. In this calculation the difference between the normalized locking signal frequency and the normalized free-running oscillator (FRO) frequency is $\delta_L=(\omega_o-\omega_{FR})/\omega_o=1.05\times10^{-3}$ or $\Delta f=35$ MHz. Figures 2(b) and 2(c) show that phase-locked operation is obtained after 30 nsec into the voltage pulse. The phase-locked condition is indicated by a frequency shift $\omega-\omega_o=0$ and constant rf phase. As shown in Figure 2(a), in this case the oscillator efficiency is reduced slightly to 16% while phase-locked.

If the difference between the locking signal frequency and the FRO frequency Δf is too large, phase-locking will not occur. Instead a periodic perturbation of the oscillator behavior is observed as shown in Figures 3(a)-3(c). The locking signal detuning in this case is $\delta_L = 1.55 \times 10^{-3}$ or $\Delta f = 54$ MHz. The beat frequency of the perturbation is about 28 MHz. The non-phase-locked behavior of the rf phase is clearly shown by Fig. 3(c).

The case of a FRO with a voltage ripple is shown in Figures 4(a)-4(c). The voltage ripple amplitude is 2% and the ripple period is 10 nsec. Other parameters are the same as for the FRO case discussed above. Figures 4(a) and 4(b) show that this voltage ripple causes a 3.4% amplitude ripple in the efficiency and a 0.06% amplitude ripple (21 MHz) in the frequency. Figures 5(a)-5(b) show the results of driving this oscillator configuration with a prebunched beam with $q_B = 0.5$ and modulation frequency shift $\delta_L = 5.5 \times 10^{-4}$ (19 MHz). Figures 5(b) and 5(c) show that phase-locked operation is achieved in the sense that after about 30 nsec the oscillation frequency averaged over the ripple period equals the drive frequency and the averaged rf phase angle is a constant. As in the FRO, the voltage ripple leads to a 0.06% frequency ripple in the PLO. The frequency ripple causes a corresponding 13° amplitude ripple in the phase angle. Figures 6(a)-6(c) represent the case of an unphase-locked, driven oscillator with a 2% voltage ripple. The drive signal frequency shift is δ_L=2.5×10^{-3} (88 MHz). The beat frequency for the perturbed oscillator is about 34 MHz. The failure to achieve phase-locked operation is clearly shown by the phase angle plotted in Figure 6(c).

To estimate the input power needed to obtain a beam bunching parameter q_B=0.5 for circularly polarized radiation and a gaussian rf profile in the bunching cavity, one can apply the small signal gyroklystron theory developed by Tran et al [20]. The required input power in Watts is:

$$P_{in}(W) = \frac{\sqrt{\pi} c^3 m_o^2 \; (x_n'^2 - m^2) \; J_m^2(x'_n) \; \gamma_o^2 \beta_{to}^4 \beta_{zo} \; q_B^2 \; e^{2x^2}}{2\sqrt{2} \mu_o e^2 \; J_{m-s}^2 (k_n R_o) \; \mu_1 \; (\sqrt{3}\mu_1 + \mu_d) \; Q_1} \tag{17}$$

where $\mu_1 = \pi\beta^2_{to} L_1/\beta_{zo}\lambda$ is the normalized interaction length of the bunching cavity, μ_d is the normalized drift length, Q_1 is the bunching cavity Q factor, and $x=(\omega_o - \Omega)L_1/4v_{zo}$ the bunching cavity magnetic field detuning parameter. The other parameters are defined above. Typical choices for μ_1 and μ_d are 2 and 3, respectively. Assuming the same mode, magnetic field and beam parameters in the bunching and power cavities, and Q_1=200, one obtains P_{in}=530 kW as the power required to phase-lock a gyrotron oscillator with an output power of over 160 MW for an effective gain of over 24 dB.

IV. CONCLUSIONS

A time slow-time-scale theory and a computer code for numerical calculations have been developed to investigate pulsed free-running and phase-locked gyrotrons. This code is expected to be a valuable resource for the design and interpretation of planned phase-locked gyrotron experiments. The calculations presented here show the feasibility of observing phase-locked operation with 50 nsec pulses. Phase-locking over a significant bandwidth is shown to be possible with a locking power 24 dB less than the oscillator output power for a single prebunching cavity. The effect of voltage ripple has been investigated and shown not to prevent phase-locked operation, however, applications requirements for rf phase control may place significant limits on allowable voltage ripple.

V. ACKNOWLEDGEMENTS

Helpful discussions with Drs. Steven Gold and John Burke are gratefully acknowledged as is the computational assistance of Lisa Lagrand. This work was supported by the Office of Innovative Science and Technology of the Strategic Defense Initiative Organization under a contract administered by the Harry Diamond Laboratories.

REFERENCES

a) JAYCOR, Inc., Vienna, VA 22180.

b) Electrical Engineering Department, University of Maryland, College Park, MD 20742.

1. P. Sprangle and W.M. Manheimer, Phys. Fluids 18, 224 (1975).
2. E. Ott and W.M. Manheimer, IEEE Trans. Plasma Sci. PS-13, 1 (1975).
3. V.A. Flyagin, A.V. Gaponov, A.V. Petelin, and V.K.Yulpatov, IEEE Trans. Microwave Theory Tech. MTT-25, 514 (1977).
4. P. Sprangle and A.T. Drobot, IEEE Trans. Microwave Theory Tech. MTT-25, 528 (1978).
5. K.R. Chu, Phys. Fluids 21, 2354 (1978).
6. K.R. Chu, A.T. Drobot, H.H. Szu, and P. Sprangle, IEEE Trans. Microwave Theory Tech. MTT-28, 313 (1980).
7. A.W. Fliflet, M.E. Read, K.R. Chu, and R. Seeley, Int. J. Electron. 53, 505 (1982).
8. B.G. Danly and R.J. Temkin, Phys. Fluids 29, 561 (1986).
9. M. Caplan, A.T. Lin, and K.R. Chu, Int. J. Electron. 53, 659 (1982).
10. M.A. Moiseev and G.S. Nusinovich, Isvestia VUZ. Radiofizika 17, 1709 (1974) [Radio Phys. Quant. Electron. 17, 1305 (1976)].

11. N.S. Ginzburg, G.S. Nusinovich, and N.A. Zavolsky, Int. J. Electron. 61, 881 (1986).

12. A. Bondeson, W.M. Manheimer, and E. Ott, Phys. FLuids 26, 285 (1983).

13. B. van der Pol, Phil. Mag. 3, 65 (1927).

14. R. Adler, Proc. Inst. Radio Engrs. 34, 351 (1946).

15. M.E. Read, R. Seeley, and W.M. Manheimer, IEEE Trans. Plasma Sci. PS-13, 398 (1985).

16. W.M. Manheimer, Int. J. Electronics 63, 29 (1987).

17. S.H. Gold, A.W. Fliflet, W.M. Manheimer, R.B. McCowan, W.M. Black, R.C. Lee, V.L. Granatstein, A.K. Kinkead, D.L. Hardesty, and M. Sucy, Phys. Fluids (to be published).

18. A.W. Fliflet, Int. J. Electron. 61, 1049 (1986).

19. T.M. Antonsen, W.M. Manheimer, and B. Levush, Int. J. Electronics 61, 823 (1986).

20. T.M. Tran, B.G. Danly, K.E.Kreischer, J.B. Schutkeker, and R.J. Temkin, Phys. Fluids 29, 1274 (1986).

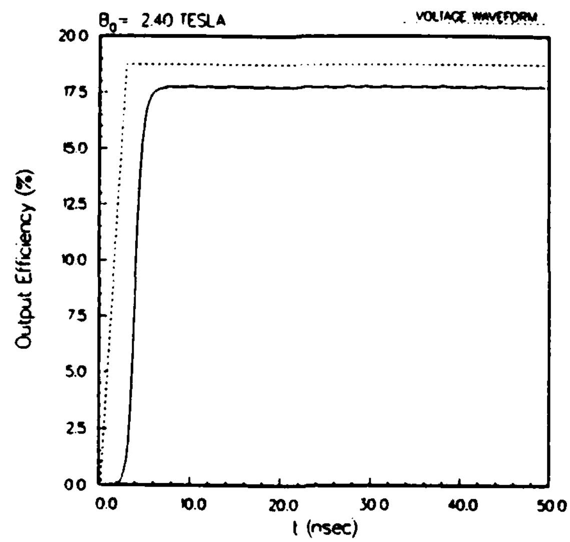

B_0 = 2.40 TESLA
VOLTAGE WAVEFORM
Output Efficiency (%)
t (nsec)

(a)

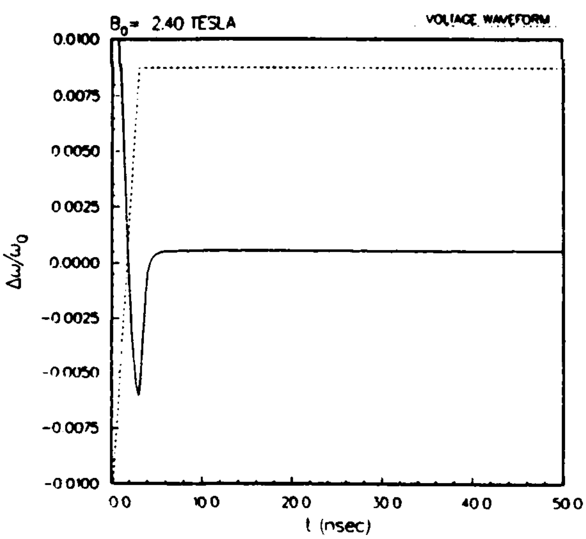

B_0 = 2.40 TESLA
VOLTAGE WAVEFORM
$\Delta\omega/\omega_0$
t (nsec)

(b)

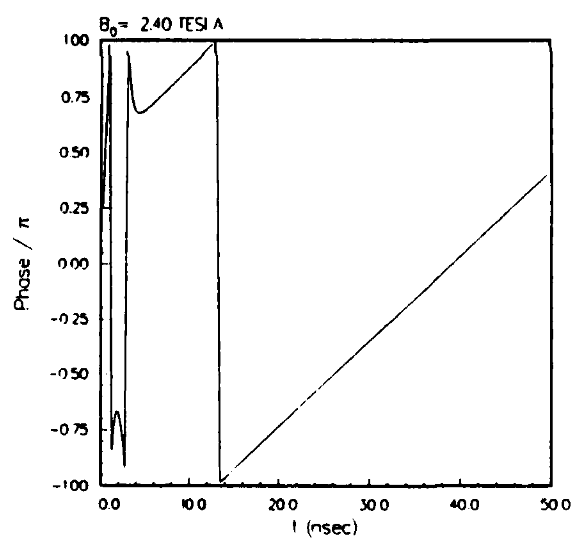

B_0 = 2.40 TESLA
Phase / π
t (nsec)

(c)

Figure 1

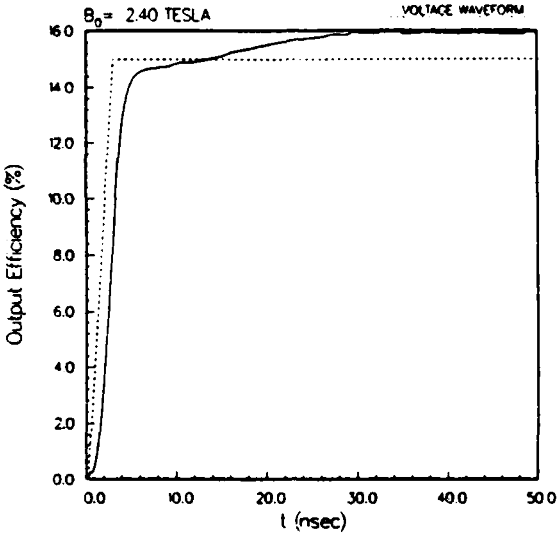

B_0= 2.40 TESLA
VOLTAGE WAVEFORM
Output Efficiency (%)
16.0
14.0
12.0
10.0
8.0
6.0
4.0
2.0
0.0
0.0
10.0
20.0
30.0
40.0
50.0
t (nsec)

(a)

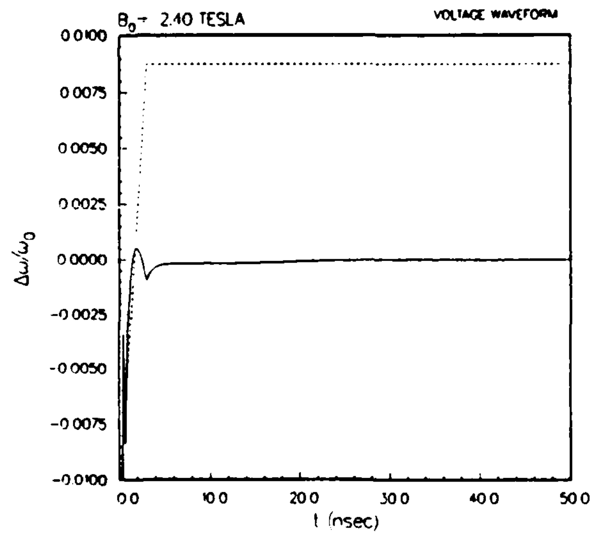

B_0= 2.40 TESLA
VOLTAGE WAVEFORM
$\Delta\omega/\omega_0$
0.0100
0.0075
0.0050
0.0025
0.0000
-0.0025
-0.0050
-0.0075
-0.0100
0.0
10.0
20.0
30.0
40.0
50.0
t (nsec)

(b)

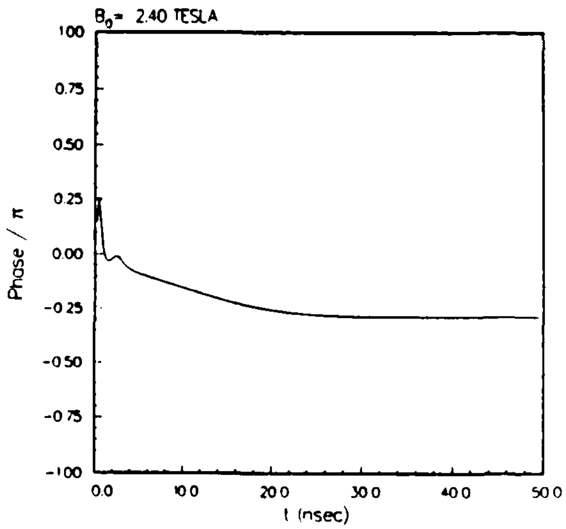

B_0= 2.40 TESLA
Phase / π
1.00
0.75
0.50
0.25
0.00
-0.25
-0.50
-0.75
-1.00
0.0
10.0
20.0
30.0
40.0
50.0
t (nsec)

(c)

Figure 2

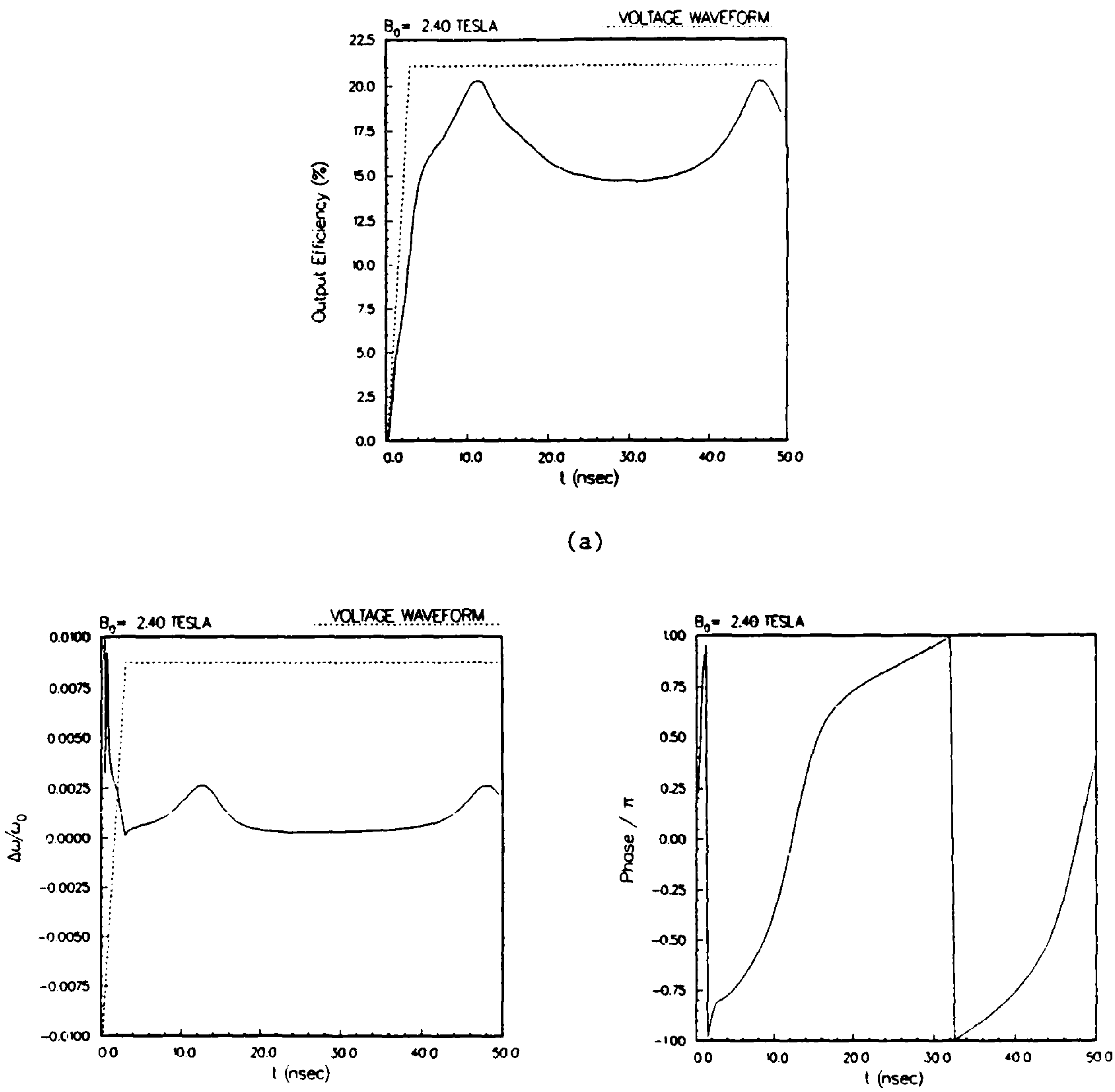

B0= 2.40 TESLA
VOLTAGE WAVEFORM
Output Efficiency (%)
t (nsec)
Δω/ω0
Phase / π

(a)

(b)

(c)

Figure 3

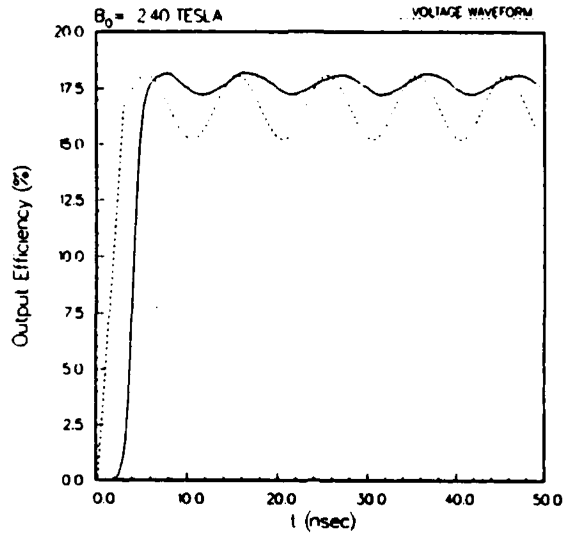
B_0 = 2.40 TESLA
VOLTAGE WAVEFORM
Output Efficiency (%)
20.0
17.5
15.0
12.5
10.0
7.5
5.0
2.5
0.0
0.0
10.0
20.0
30.0
40.0
50.0
t (nsec)

(a)

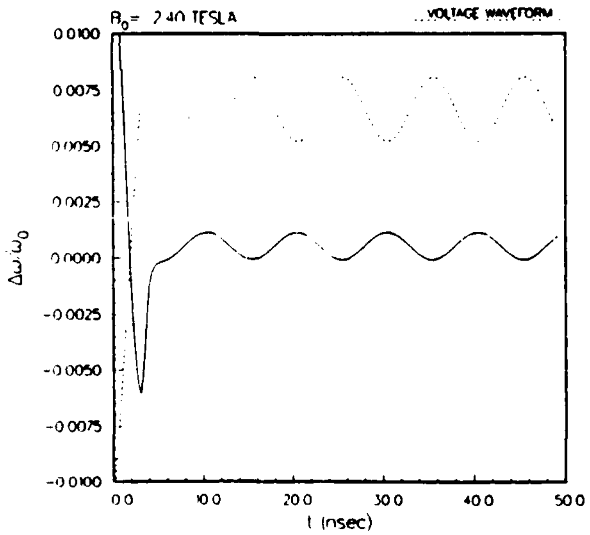
B_0 = 2.40 TESLA
VOLTAGE WAVEFORM
$\Delta\omega/\omega_0$
0.0100
0.0075
0.0050
0.0025
0.0000
-0.0025
-0.0050
-0.0075
-0.0100
0.0
10.0
20.0
30.0
40.0
50.0
t (nsec)

(b)

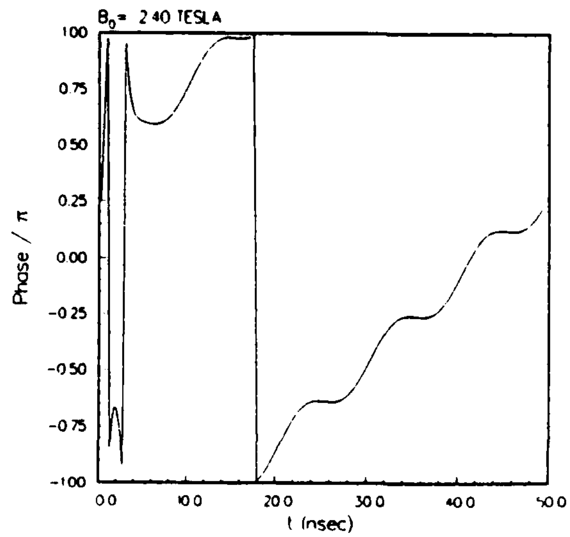
B_0 = 2.40 TESLA
Phase / π
1.00
0.75
0.50
0.25
0.00
-0.25
-0.50
-0.75
-1.00
0.0
10.0
20.0
30.0
40.0
50.0
t (nsec)

(c)

Figure 4

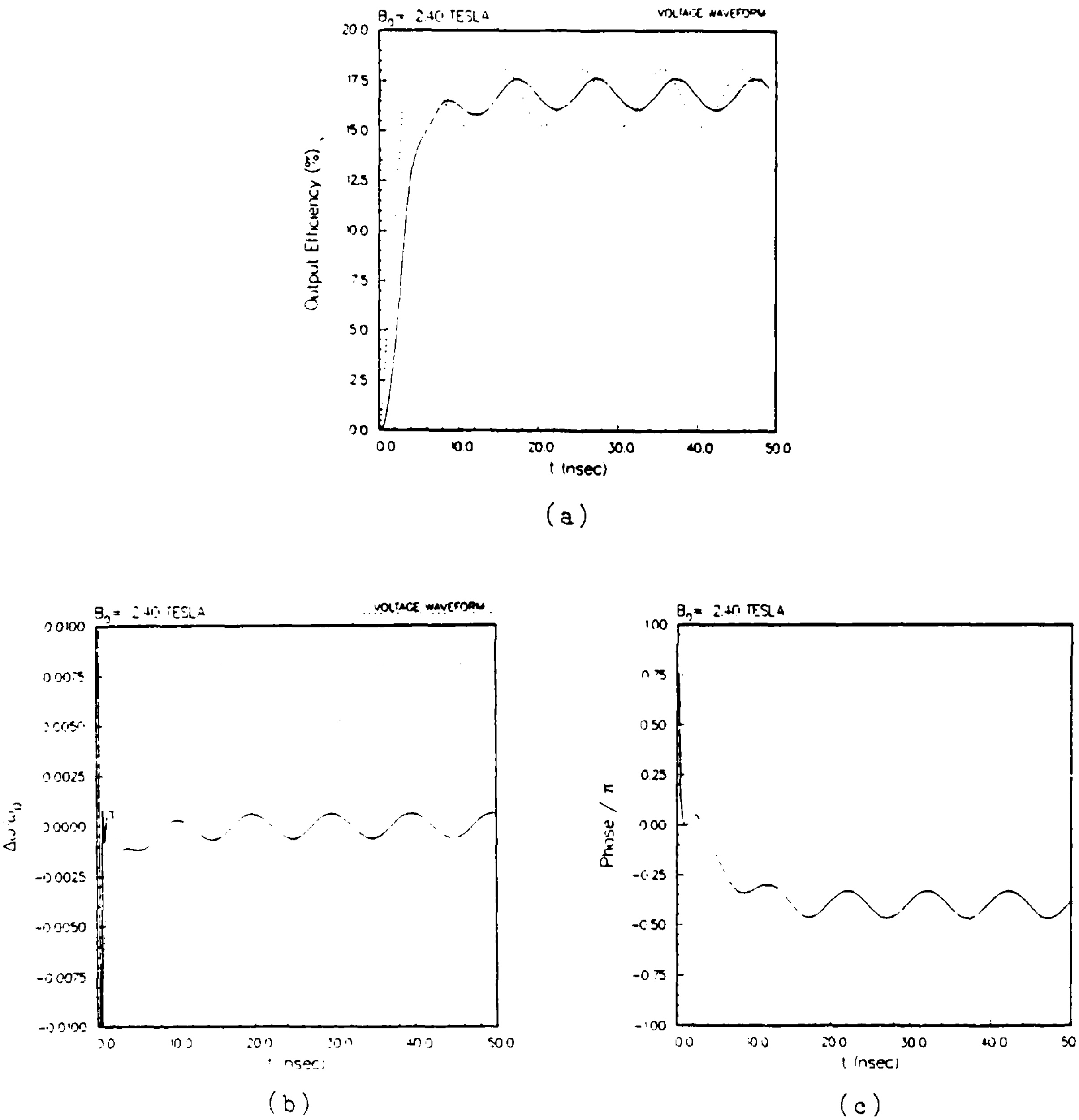

B0 = 2.40 TESLA
VOLTAGE WAVEFORM
Output Efficiency (%)
t (nsec)
(a)
B0 = 2.40 TESLA
VOLTAGE WAVEFORM
t (nsec)
(b)
B0 = 2.40 TESLA
Phase / π
t (nsec)
(c)

Figure 5

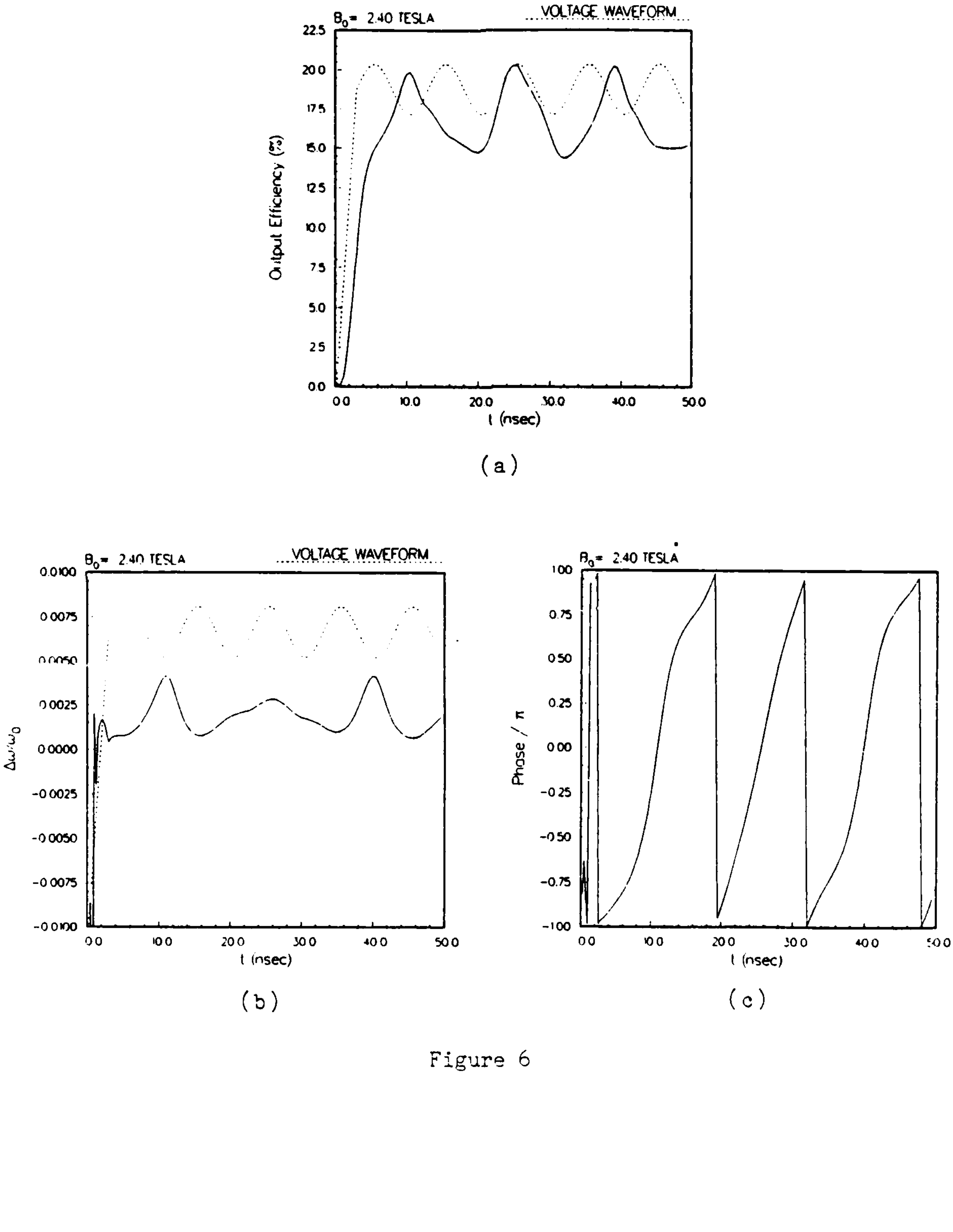

B_0= 2.40 TESLA
VOLTAGE WAVEFORM
Output Efficiency (%)
t (nsec)
(a)
$\Delta\omega/\omega_0$
(b)
Phase / π
(c)

Figure 6

4740 DISTRIBUTION LIST
(for 4740 memos)

Air Force Avionics Laboratory AFWAL/AADM-1 Wright/Patterson AFB, Ohio 45433 Attn: Walter Friez	1 copy
Air Force Office of Scientific Research Bolling AFB Washington, D.C. 20332 Attn: H. Schlossberg	1 copy
Air Force Weapons Lab Kirkland AFB Albuquerque, New Mexico 87117 Attn: Dr. William Baker	1 copy
Columbia University 520 West 120th Street Department of Electrical Engineering New York, N.Y. 10027 Attn: Dr. S.P. Schlesinger	1 copy
Columbia University 520 West 120th Street Department of Applied Physics and Nuclear Engineering New York, New York 10027 Attn: T.C. Marshall	1 copy
Cornell University School of Applied and Engineering Physics Ithica, New York 14853 Attn: Prof. Hans H. Fleischmann	1 copy
John Nation	1 copy
R. N. Sudan	1 copy
Dartmouth College 18 Wilder, Box 6127 Hanover, New Hampshire 03755 Attn: Dr. John E. Walsh	1 copy
Department of Energy Washington, D.C. 20545 Attn: C. Finfgeld/ER-542, GTN	1 copy
T.V. George/ER-531, GTN	1 copy
D. Crandall/ER-55, GTN	1 copy

Defense Advanced Research Project Agency/DEO
1400 Wilson Blvd.
Arlington, Virginia 22209
Attn: Dr. S. Shey 1 copy
Dr. L. Buchanan 1 copy

Defense Communications Agency
Washington, D.C. 20305
Attn: Dr. Pravin C. Jain
Assistant for Communications
Technology 1 copy

Defense Nuclear Agency
Washington, D.C. 20305
Attn: Mr. J. Farber 1 copy
Maj. J. Benson 1 copy
Capt. D. Stone 1 copy
Mr. Lloyd Stossell 1 copy

Defense Technical Information Center
Cameron Station
5010 Duke Street
Alexandria, Virginia 22314 2 copies

Georgia Tech. EES-EOD
Baker Building
Atlanta, Georgia 30332
Attn: Dr. James J. Gallagher 1 copy

Hanscomb Air Force Base
Stop 21, Massachusetts 01731
Attn: Lt. Rich Nielson/ESD/INK 1 copy

Hughes Aircraft Co.
Electron Dynamics Division
3100 West Lomita Boulevard
Torrance, California 90509
Attn: J. Christiansen 1 copy
J.J. Tancredi 1 copy

KMS Fusion, Inc.
3941 Research Park Dr.
P.O. Box 1567
Ann Arbor, Michigan 48106
Attn: S.B. Segall 1 copy

Lawrence Livermore National Laboratory
P.O. Box 808
Livermore, California 94550
Attn: Dr. D. Prosnitz 1 copy
Dr. T.J. Orzechowski 1 copy
Dr. J. Chase 1 copy

Los Alamos Scientific Laboratory
P.O. Box 1663, AT5-827
Los Alamos, New Mexico 87545

Attn: Dr. J.C. Goldstein	1 copy
Dr. T.J.T. Kwan	1 copy
Dr. L. Thode	1 copy
Dr. C. Brau	1 copy
Dr. R. R. Bartsch	1 copy

Massachusetts Institute of Technology
Department of Physics
Cambridge, Massachusetts 02139

Attn: Dr. G. Bekefi/36-213	1 copy
Dr. M. Porkolab/NW 36-213	1 copy
Dr. R. Davidson/NW 16-206	1 copy
Dr. A. Bers/NW 38-260	1 copy
Dr. K. Kreischer	1 copy

Massachusetts Institute of Technology
167 Albany St., N.W. 16-200
Cambridge, Massachusetts 02139

Attn: Dr. R. Temkin/NW 14-4107	1 copy

Spectra Technologies
2755 Northup Way
Bellevue, Washington 98004

Attn: Dr. J.M. Slater	1 copy

Mission Research Corporation
Suite 201
5503 Cherokee Avenue
Alexandria, Virginia 22312

Attn: Dr. M. Bollen	1 copy
Dr. Tom Hargreaves	1 copy

Mission Research Corporation
1720 Randolph Road, S.E.
Albuquerque, New Mexico 87106

Attn: Dr. Ken Busby	1 copy
Mr. Brendan B. Godfrey	1 copy

SPAWAR
Washington, D.C. 20363
Attn: E. Warden

Code PDE 106-3113	1 copy

Naval Research Laboratory
Addressee: Attn: Name/Code

Code 1001 - T. Coffey	1 copy
CODE 1220 - Security	1 copy
Code 2628 - TID Distribution	22 copies
Code 4000 - W. Ellis	1 copy
Code 4700 - S. Ossakow	26 copies

Code 4700.1 - A.W. Ali	1 copy
Code 4710 - C. Kapetanakos	1 copy
Code 4740 - Branch Office	25 copies
Code 4740 - W. Black	1 copy
Code 4740 - A. Fliflet	1 copy
Code 4740 - S. Gold	1 copy
Code 4740 - A. Kinkead	1 copy
Code 4740 - W.M. Manheimer	1 copy
Code 4740 - M.E. Read	1 copy
Code 4740 - M. Rhinewine	1 copy
Code 4770 - G. Cooperstein	1 copy
Code 4790 - B. Hui	1 copy
Code 4790 - C.M. Hui	1 copy
Code 4790 - Y.Y. Lau	1 copy
Code 4790 - P. Sprangle	1 copy
Code 5700 - L.A. Cosby	1 copy
Code 6840 - S.Y. Ahn	1 copy
Code 6840 - A. Ganguly	1 copy
Code 6840 - R.K. Parker	1 copy
Code 6840 - N.R. Vanderplaats	1 copy
Code 6850 - L.R. Whicker	1 copy
Code 6875 - R. Wagner	1 copy

Naval Sea Systems Command
Department of the Navy
Washington, D.C. 20362
Attn: Commander George Bates
PMS 405-300 — 1 copy

Northrop Corporation
Defense Systems Division
600 Hicks Rd.
Rolling Meadows, Illinois 60008
Attn: Dr. Gunter Dohler — 1 copy

Oak Ridge National Laboratory
P.O. Box Y
Mail Stop 3
Building 9201-2
Oak Ridge, Tennessee 37830
Attn: Dr. A. England — 1 copy

Office of Naval Research
800 N. Quincy Street
Arlington, Va. 22217
Attn: Dr. C. Roberson — 1 copy
Dr. W. Condell — 1 copy
Dr. T. Berlincourt — 1 copy

Office of Naval Research
1030 E. Green Street
Pasadena, CA 91106
Attn: Dr. R. Behringer — 1 copy

Optical Sciences Center University of Arizona Tucson, Arizona 85721 Attn: Dr. Willis E. Lamb, Jr.	1 copy
OSD/SDIO Attn: IST (Dr. H. Brandt) Washington, D.C. 20301-7100	1 copy
Pacific Missile Test Center Code 0141-5 Point Muga, California 93042 Attn: Will E. Chandler	1 copy
Physical Dynamics, Inc. P.O. Box 10367 Oakland, California 94610 Attn: A. Thomson	1 copy
Physics International 2700 Merced Street San Leandro, California 94577 Attn: Dr. J. Benford	1 copy
Princeton Plasma Plasma Physics Laboratory James Forrestal Campus P.O. Box 451 Princeton, New Jersey 08544 Attn: Dr. H. Hsuan	2 copies
Dr. J. Doane	1 copy
Quantum Institute University of California Santa Barbara, California 93106 Attn: Dr. L. Elias	1 copy
Raytheon Company Microwave Power Tube Division Foundry Avenue Waltham, Massachusetts 02154 Attn: N. Dionne	1 copy
Sandia National Laboratories ORG. 1231, P.O. Box 5800 Albuquerque, New Mexico 87185 Attn: Dr. Thomas P. Wright	1 copy
Mr. J.E. Powell	1 copy
Dr. J. Hoffman	1 copy
Dr. W.P. Ballard	1 copy
Dr. C. Clark	1 copy

Science Applications, Inc.
1710 Goodridge Dr.
McLean, Virginia 22102
Attn: Adam Drobot 1 copy
P. Vitrello 1 copy

Stanford University
High Energy Physics Laboratory
Stanford, California 94305
Attn: Dr. T.I. Smith 1 copy

TRW, Inc.
Space and Technology Group
Suite 2600
1000 Wilson Boulevard
Arlington, VA 22209
Attn: Dr. Neil C. Schoen 1 copy

TRW, Inc.
Redondo Beach, California 90278
Attn: Dr. H. Boehmer 1 copy
Dr. T. Romisser 1 copy

University of California
Physics Department
Irvine, California 92717
Attn: Dr. G. Benford 1 copy
Dr. N. Rostoker 1 copy

University of California
Department of Physics
Los Angeles, CA 90024
Attn: Dr. A.T. Lin 1 copy
Dr. N. Luhmann 1 copy
Dr. D. McDermott 1 copy

University of Maryland
Department of Electrical Engineering
College Park, Maryland 20742
Attn: Dr. V. L. Granatstein 1 copy
Dr. W. W. Destler 1 copy

University of Maryland
Laboratory for Plasma and Fusion
Energy Studies
College Park, Maryland 20742
Attn: Dr. Jhan Varyan Hellman 1 copy
Dr. John McAdoo 1 copy
Dr. John Finn 1 copy
Dr. Baruch Levush 1 copy
Dr. Tom Antonsen 1 copy
Dr. Edward Ott 1 copy

University of Tennessee
Dept. of Electrical Engr.
Knoxville, Tennessee 37916
Attn: Dr. I. Alexeff — 1 copy

University of New Mexico
Department of Physics and Astronomy
800 Yale Blvd, N.E.
Albuquerque, New Mexico 87131
Attn: Dr. Gerald T. Moore — 1 copy

University of Utah
Deparment of Electrical Engineering
3053 Merrill Engineering Bldg.
Salt Lake City, Utah 84112
Attn: Dr. Larry Barnett — 1 copy
Dr. J. Mark Baird — 1 copy

U. S. Naval Academy
Annapolis, Maryland 21402-5021 — 1 copy

U. S. Army
Harry Diamond Labs
2800 Powder Mill Road
Adelphi, Maryland 20783-1145
Attn: Dr. Edward Brown — 1 copy
Dr. Michael Chaffey — 1 copy

Varian Associates
611 Hansen Way
Palo Alto, California 94303
Attn: Dr. H. Jory — 1 copy
Dr. David Stone — 1 copy
Dr. Kevin Felch — 1 copy
Dr. A. Salop — 1 copy

Yale University
Applied Physics
Madison Lab
P.O. Box 2159
Yale Station
New Haven, Connecticut 06520
Attn: Dr. N. Ebrahim — 1 copy
Dr. I. Bernstein — 1 copy

Director of Research
U.S. Naval Academy
Annapolis, MD 21402 2Copies

Code 1220 1 Copy

END
FILMED
MARCH, 1988
DTIC